M.Sc. Report – Option II:

Fate of entanglement in surface codes

Lucy Liuxuan Zhang
Department of Physics
University of Toronto

July 31, 2007

Abstract

Acknowledgements

Contents

1 Introduction **1**

2 Two-qubit entanglement **2**

2.1 Separability . . . 2

2.1.1 State tomography . . . 2

2.1.2 Partial transpose . . . 2

2.1.3 Witness . . . 2

2.2 Meausure of entanglement . . . 2

2.2.1 Entanglement of formation . . . 2

2.2.2 Concurrence . . . 2

3 Surface codes **3**

3.1 Construction . . . 3

3.2 Challenge of fault-tolerant recovery . . . 6

3.3 Error model . . . 6

3.4 Modelling errors and syndromes . . . 7

3.5 Recovery . . . 8

3.6 Threshold and estimates . . . 8

4 Matching **10**

4.1 Basic definitions . . . 10

4.2 Minimum-weight perfect matching . . . 10

4.3 Edmond's algorithm . . . 10

4.4 Linear porgramming . . . 10

5 Simulation **11**

6 Results **12**

7 Conclusion **13**

List of Figures

3.1 Diagram verbatim from Dennis et al. [2002]. On an 8×8 toric lattice, the logical operators $\overline{X}_i$ and $\overline{Z}_i$ ($i = 1, 2$) act nontrivially on a homologically nontrivial chain of links with local X and Z operators respectively. In (a), the anticommuting operators $\overline{X}_1$ and $\overline{Z}_1$ act on the same logical qubit, say the first one. And the anticommuting operations $\overline{X}_2$ and $\overline{Z}_2$ in (b) act on the second logical qubit. 5

3.2 Diagram verbatim from Dennis et al. [2002]. Error chains and syndromes in the absence of measurement errors. The actual error chain is shown as darkened links, and defects as grey dots. 7

3.3 Diagram verbatim from Dennis et al. [2002]. Map of syndromes and measurement errors. The partially shaded site indicates the location of a missing defect, which is also a genuine defect. Since measurement errors are present, we have ghost defects as well as genuine defects, some of which might be "missing". The detected (nontrivial) syndrome includes both the non-missing genuine defects and the ghost defects while it should include only the genuine defects. 8

3.4 Diagram verbatim from Dennis et al. [2002]. Map of syndromes and measurement errors. The partially shaded site indicates the location of a missing defect, which is also a genuine defect. Since measurement errors are present, we have ghost defects as well as genuine defects, some of which might be "missing". The detected (nontrivial) syndrome includes both the non-missing genuine defects and the ghost defects while it should include only the genuine defects. 9

Chapter 1

Introduction

cite Preskill

Chapter 2

Two-qubit entanglement

2.1 Separability

2.1.1 State tomography

2.1.2 Partial transpose

2.1.3 Witness

2.2 Meausure of entanglement

2.2.1 Entanglement of formation

2.2.2 Concurrence

Chapter 3

Surface codes

In this section, we study the error recovery for surface codes, which was introduced by Kitaev [2003], after a brief review of its construction. More detailed constructions of the toric code and the planar code, as well as the homological ideas for analyzing the errors in the case of perfect syndrome measurements, have been given in my earlier term paper [Zhang, 2005]. Our discussion here about surface codes is again focused on the simpler cases of the toric code and the planar surface code. According to Dennis et al. [2002], the accuracy thresholds for the two codes are the same, therefore we shall assume below that we are working with a toric code unless otherwise stated.

3.1 Construction

Recall that a toric code is defined on an $L \times L$ lattice where the left edge is identified with the right edge, and the top with the bottom, with the appropriate orientation. So the setting is an $L \times L$ lattice layed out on a torus. However, it is often more convenient to represent it on a plane with periodic boundary conditions. On each edge of the lattice, there resides one qubit. Hence there are $n = 2L^2$ qubits on the lattice counting both the vertical and horizontal types of links. The stabilizer generators (check operators) for the toric code are the local (on the torus) site and plaquette operators of the form

$$X_s = \bigotimes_{l \ni s} X_l \qquad \text{and} \qquad Z_P = \bigotimes_{l \in P} Z_l \tag{3.1}$$

respectively, defined on each site s and plaquette P of the lattice. A site operator X_s acts nontrivially on the four links for which the site s is an endpoint whereas a plaquette operator Z_P acts nontrivially on the four links which form the sides of the plaquette P. It is easy to see that this set of check operators commute because the same type of operators trivially commute, and the number of links acted on nontrivially by any two operators of different types is always even. Due to the periodic boundary condition, the L^2 check operators are not all independent. In fact, any site (plaquette) operator can be written as a product of the remaining site (plaquette) operators since we have

$$\prod_s X_s = I^{\otimes n} \qquad \text{and} \qquad \prod_P Z_P = I^{\otimes n} \tag{3.2}$$

where the products are taken over all sites and plaquettes respectively. Equations 3.2 arise from the fact that any edge touches two sites and lies between two plaquettes, and $X^2 = I = Z^2$. Furthermore, there are no other independent relations amongst these check operators because for a nontrivial product of check operators to act trivially on all links, the inclusion of one site (plaquette) operator in the product implies the inclusion of all of its neighbouring site (plaquette) operators, eventually demanding all site (plaquette) operators to be included. Therefore, we have $2(L^2-1)$ independent stabilizer generators, and the toric code encodes $2L^2 - 2(L^2-1) = 2$ qubits. Since the shortest nontrivial homology cycle on the torus consists of L links, the minimum weight operator(s) in the normalizer has weight L. Putting these arguements together, we obtain the following.

Theorem 3.1.1. The toric code on an $L \times L$ lattice is a $[2L^2, 2, L]$ quantum error correcting code.

The syndrome is given by the measurement outcomes of all independent check operators (generators of the stabilizer). A state defined on the lattice is in the codespace if and only if the syndrome is normal (trivial). Hence, the codespace is the simultaneous $+1$ eigenspace of all check operators. For the toric code, this simultaneous eigenspace is a four-dimensional complex Hilbert space. An error recovery procedure takes any state defined on the toric lattice into the codespace while fixing the codewords.

The logical X and logical Z operators on the two encoded qubits are chosen to be the four operators shown in Figure 3.1.

We can justify our choice of the logical operators. First, note that these operators indeed take a codeword to a codeword since they commute with the check operators. For instance, for the logical operator $\overline{X}_1$, we have

$$P\overline{X}_1|\psi\rangle = \overline{X}_1 P|\psi\rangle = \overline{X}_1|\psi\rangle \tag{3.3}$$

for any ψ in the codespace and P in the stabilizer. However, they are not in the stabilizer, hence acting nontrivially on the logical qubit. Furthermore, these logical operators act independently on the codespace, and satisfy the appropriate commutation relations.

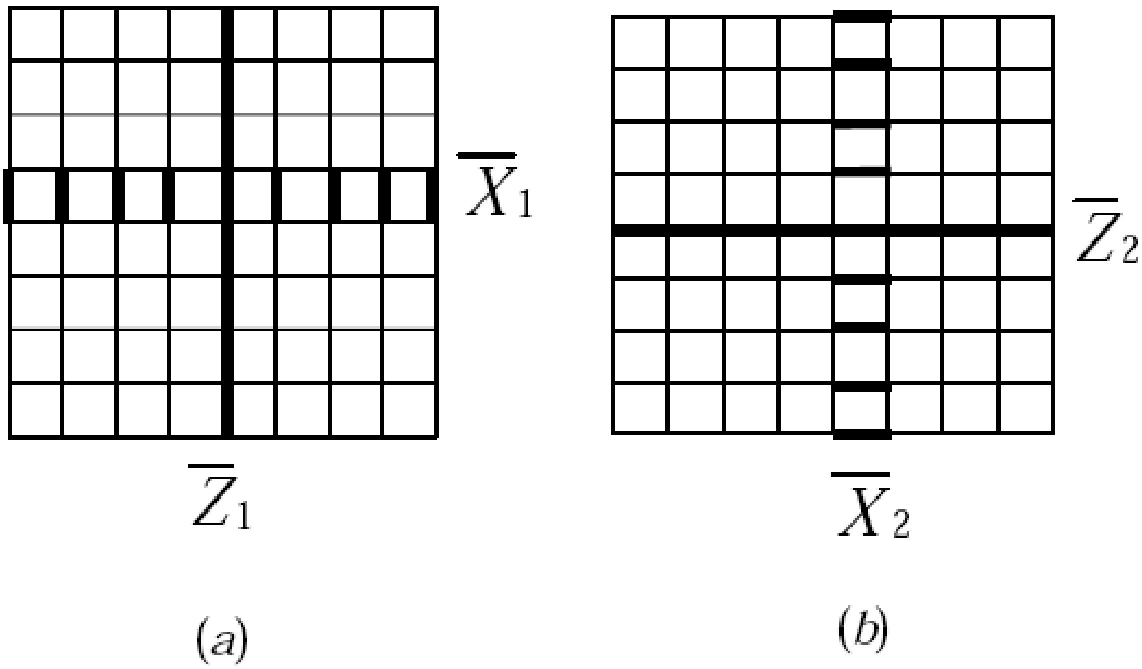

Figure 3.1: Diagram verbatim from Dennis et al. [2002]. On an 8×8 toric lattice, the logical operators $\overline{X}_i$ and $\overline{Z}_i$ $(i = 1, 2)$ act nontrivially on a homologically nontrivial chain of links with local X and Z operators respectively. In (a), the anticommuting operators $\overline{X}_1$ and $\overline{Z}_1$ act on the same logical qubit, say the first one. And the anticommuting operations $\overline{X}_2$ and $\overline{Z}_2$ in (b) act on the second logical qubit.

3.2 Challenge of fault-tolerant recovery

As discussed in [Dennis et al., 2002], fault-tolerant recovery for a surface code is a subtle matter. Not only do we have to correctly guess error chains given a syndrome, the syndrome measurements themselves might also be erroneous. In that case, we need to repeat syndrome measurements to get reliable syndromes. In the following subsections, we shall describe the syndrome analysis for both cases. Once we have correctly guessed an error chain, we can recover the codeword by performing local unitaries in parallel. Errors in the correction procedure, however, is not dealt with here. We shall arrive at an estimated accuracy threshold based on the fidelity of the guessed error chain.

3.3 Error model

Our error model for the recovery discussion here consists of errors on the data qubits and errors on the measurement outcomes. Imagine that in each time step, we measure all check operators while new errors might occur on our data. Let us assume that within every time step, bit-flip (X) errors and phase (Z) errors occur on each qubit with equal probability p, and that these errors are uncorrelated. Thus, any qubit in a state ρ undergoes

$$\rho \to \rho' = (1-p)^2 I\rho I + p(1-p)X\rho X + p(1-p)Z\rho Z + p^2 Y\rho Y \tag{3.4}$$

in the mean time. Furthermore, we assume that the syndrome bits are faulty in an uncorrelated manner with probability q. Recall that the syndrome bits are given by the measurement outcomes of the independent check operators.

The quantum channel (Equation 3.4) which a qubit goes through in each time step involves all three types of Pauli errors, namely X, Y and Z. To deal such an error model, however, we need only show that pure X errors and pure Z errors can be dealt with separately for the following reasons. Given an initial qubit mixed state ρ, with a decomposition $\{p_i, \psi_i\}_i$, the output state ρ' can be decomposed into an ensemble of the form $\{p_{ij}, \sigma_j \psi_i\}_{i,j}$ where

$$\{\sigma_0, \sigma_1, \sigma_2, \sigma_3\} = \{I, X, Y, Z\} \quad \text{and} \quad p_{ij} = \begin{cases} p_i\,(1-p)^2 & \text{if } i = 0 \\ p_i\,p(1-p) & \text{if } i = 1, 3 \\ p_i\,p^2 & \text{if } i = 2. \end{cases} \tag{3.5}$$

Some of the pure states in this ensemble might be the same, in which case, we can combine

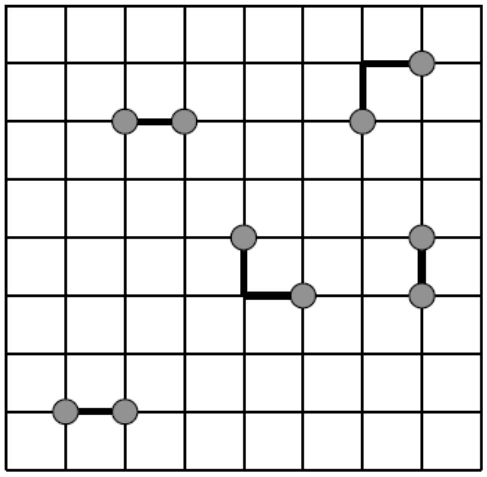

Figure 3.2: Diagram verbatim from Dennis et al. [2002]. Error chains and syndromes in the absence of measurement errors. The actual error chain is shown as darkened links, and defects as grey dots.

their probabilities. The code can restore ρ' to ρ if and only if it can restore every pure state $\sigma_j \psi_i$ in the final mixture to ψ_i. Furthermore, since $Y = iXZ$,

If the code can correct every pure state in the ensemble, then it can correct **HERE** Calderbank-Shor-Steane codes.

3.4 Modelling errors and syndromes

As a first step towards error recovery, we try to understand the interactions between the syndromes and error chains.

repetition **HERE** For the moment, let us deal only with Z errors. Then we need only measure the site operators to obtain the syndrome since the plaquette operators commute with any local Z operators, always yielding trivial syndrome bits.

In the absence of measurement errors, we obtain after a syndrome measurement the locations of abnormal syndrome bits corresponding to the endpoints of the actual error chain, which we call the *defects*, as shown in Figure 3.2. Since errors on different qubits are uncorrelated and occur with equal probability p, short error chains are more likely. Therefore, we can guess a shortest error chain in agreement with the given syndrome for the recovery.

However, in the general case where syndrome measurements are imperfect, we also have "ghost defects", where the measured syndrome bits indicate a defect even though

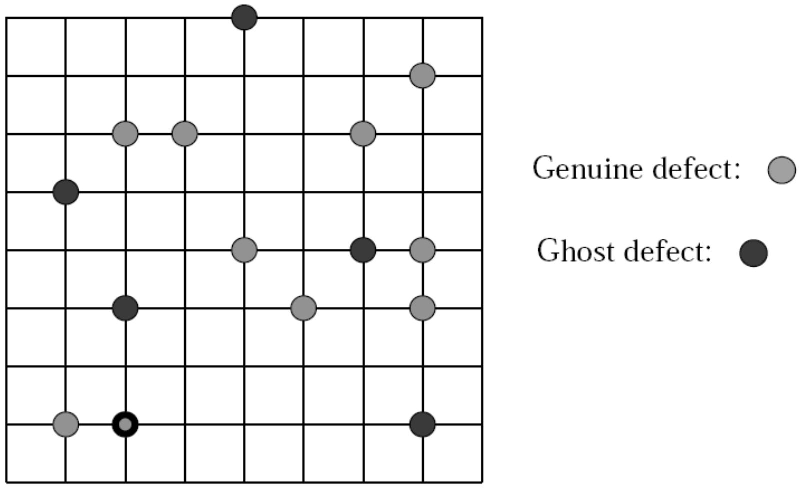

Figure 3.3: Diagram verbatim from Dennis et al. [2002]. Map of syndromes and measurement errors. The partially shaded site indicates the location of a missing defect, which is also a genuine defect. Since measurement errors are present, we have ghost defects as well as genuine defects, some of which might be "missing". The detected (nontrivial) syndrome includes both the non-missing genuine defects and the ghost defects while it should include only the genuine defects.

no defect is actually present there, and "missing defects", where actual defects go unobserved. The situation is thus much more complicated as illustrated in Figure 3.3.

To deal with this complication a third dimension to the lattice, which corresponds to time.

Stacking these time slices together in temporal order then gives defects in spacetime as shown in repetition

3.5 Recovery

3.6 Threshold and estimates

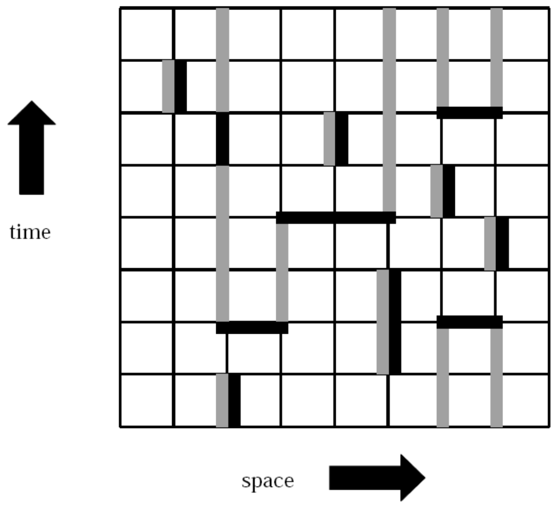

Figure 3.4: Diagram verbatim from Dennis et al. [2002]. Map of syndromes and measurement errors. The partially shaded site indicates the location of a missing defect, which is also a genuine defect. Since measurement errors are present, we have ghost defects as well as genuine defects, some of which might be "missing". The detected (nontrivial) syndrome includes both the non-missing genuine defects and the ghost defects while it should include only the genuine defects.

Chapter 4

Matching

4.1 Basic definitions

4.2 Minimum-weight perfect matching

4.3 Edmond's algorithm

4.4 Linear porgramming

Chapter 5

Simulation

Chapter 6

Results

Chapter 7

Conclusion

something here

Appendix A: Stabilizer formalism

Bibliography

E. Dennis, A. Kitaev, A. Landahl, and J. Preskill. Topological quantum memory. *Journal of Mathematical Physics*, 43:4452–4505, September 2002. doi: 10.1063/1.1499754.

A. Y. Kitaev. Fault-tolerant quantum computation by anyons. *Annals of Physics*, 303: 2–30, January 2003.

L. L. Zhang. Understanding surface quantum error-correcting codes. 2005.